Photo-induced insulator–metal transition probed by Raman spectroscopy

2009 J. Phys.: Condens. Matter 21 075603

(http://iopscience.iop.org/0953-8984/21/7/075603)

J. Phys.: Condens. Matter **21** (2009) 075603 (6pp) doi:10.1088/0953-8984/21/7/075603

Photo-induced insulator–metal transition probed by Raman spectroscopy

V G Sathe[1], R Rawat[1], Aditi Dubey[1], A V Narlikar[1] and D Prabhakaran[2]

[1] UGC-DAE Consortium for Scientific Research, University Campus, Khandwa Road, Indore 452017, India
[2] Department of Physics, Clarendon Laboratory, University of Oxford, Oxford OXI 3PU, UK

Received 13 October 2008, in final form 12 December 2008
Published 29 January 2009
Online at stacks.iop.org/JPhysCM/21/075603

Abstract
Strongly correlated electron systems give an opportunity to manipulate charge, orbital, magnetic and structural phases of matter. Here we show that the insulating phase where charges are localized can be delocalized through photo-excitation which, in turn changes the structure locally, inducing an orthorhombic to rhombohedral phase transition. The I–M transition was witnessed for $La_{1-x}Sr_xMnO_3$ compounds in Raman spectra and photo-induced conduction simultaneously. A simple continuous argon ion laser source was used for optical excitation. The photon energy was 2.53 eV and the power can be chosen anywhere between 5 and 45 mW. Our studies clearly bring out the role of local disorder in the form of Jahn–Teller distortion in the localization of electrons.

(Some figures in this article are in colour only in the electronic version)

1. Introduction

$La_{1-x}Sr_xMnO_3$ is a perovskite manganite with small structural distortions around Mn–O_6 octahedra that drives the system from its ideal cubic structure. Another factor that is coupled with the structural change is the doping concentration x. It undergoes an orthorhombic (space group $Pnma$) to rhombohedral ($R\bar{3}c$) structural transition on increasing doping concentration and/or with variation in temperature [1, 2]. This system shows a variety of ground states from antiferromagnetic insulator (for $x < 0.1$) to ferromagnetic insulator with orbital order ($0.1 \leqslant x < 0.16$) to ferromagnetic metallic state [3]. This system has very strong coupling between the charge carriers, localized spin moments of the manganese and the lattice structure. This coupling is manifested in the structural phase transition on application of a magnetic field [2]. The main cause of such a structural transformation is attributed to a change of tolerance factor of the perovskite-like structure [4]. The tolerance factor gives a measure of deviation of the Mn–O–Mn bond angle from 180°. The deviation is larger in the orthorhombic structure leading to charge localization when compared to the rhombohedral lattice. Thus, the lattice degree of freedom is expected to couple with the kinetic energy of the conduction e_g electron and hole carriers. To understand the mechanisms of the colossal magnetoresistance, many attempts were made taking into account the strong interplay of magnetism, electron–lattice coupling, and orbital and charge ordering in these materials. It was shown earlier that double exchange alone cannot explain the large magnetoresistance in these materials [5]. However, the details of the physical mechanisms responsible for different transitions are not yet well understood. Present understanding about the phenomena considers the collapse of a phase, coexisting and competing with other phases, into a energetically more favourable state which is triggered by an external stimuli like magnetic field, electric field, etc [6–8]. The insulator to metal transition induced by any small perturbation like a magnetic field [1], x-rays [9], visible photons [10–12], current [13] and even acoustic pulses [4] signifies that a large number of mechanisms of similar energies are simultaneously active in this system involving strong correlations among lattice, charge, orbital and electronic degrees of freedom.

In this paper we show strong correlation among lattice and electronic degrees of freedom in the photo-induced insulator–metal transition. We also show that the lattice excitations can be triggered by impulsive stimulated Raman scattering illuminated by a CW laser.

We carried out Raman and resistivity measurements at room temperature on single crystals of $La_{1-x}Sr_xMnO_3$; $x = 0.0, 0.05, 0.1, 0.3, 0.5$ samples showing a photo-induced insulator–metal transition. Raman spectroscopy gives information about the phonons in the material that is related

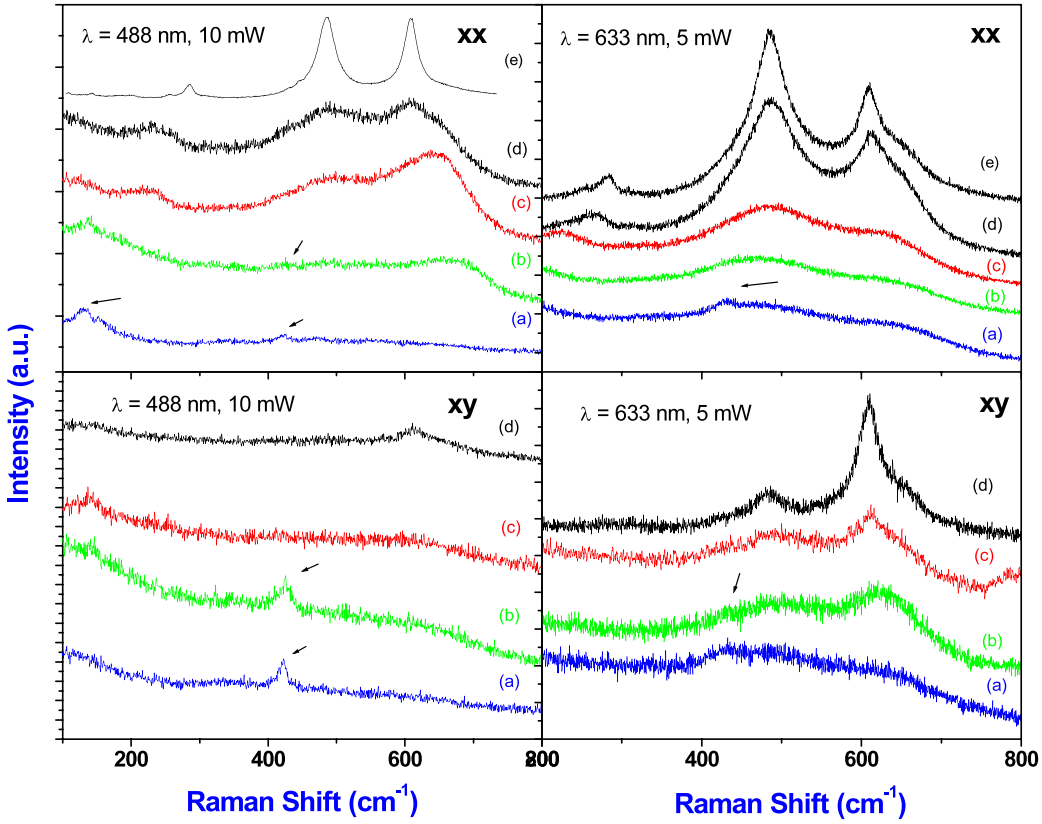

Figure 1. Raman spectra of $La_{1-x}Sr_xMnO_3$ single crystals (a) $x = 0.5$, (b) $x = 0.3$, (c) $x = 0.1$, (d) $x = 0.05$ and (e) $x = 0.0$; collected in parallel (xx) and cross-polarization (xy) mode using 488 nm (left) and 632.8 nm (right) excitation wavelengths at 300 K. The spectra are shifted upwards for clarity. The arrow denotes the extra peaks seen only in $x = 0.3$ and 0.5 samples that are metallic in nature at room temperature.

to the lattice structure. This enables the study of strong correlations among lattice degrees of freedom with magnetic order, charge order, orbital order and electronic localization–delocalization present in $La_{1-x}Sr_xMnO_3$ compounds.

2. Experimental details

Polycrystalline $La_{1-x}Sr_xMnO_3$ was synthesized by the conventional solid-state reaction using high purity La_2O_3, $SrCO_3$ and MnO_2 chemicals. Single crystals were grown using the sintered polycrystalline rod by an optical floating-zone furnace under a controlled atmosphere [14]. The Raman measurements were performed using a LabRam HR 800 Micro-Raman instrument with either a 9 mW HeNe (632.8 nm) or argon 5–45 mW (variable power) (488 nm) laser as an excitation source focused into a $\sim$1 μm diameter spot in a backscattering geometry, where the incident beam is linearly polarized and the spectral detection is unpolarized or polarized in XX and XY directions, where X and Y represent the [100] and [010] directions of the pseudo-cubic unit cell of a $La_{1-x}Sr_xMnO_3$ crystal that is perpendicular to the incident beam. An Mplan 50× lens was used during the entire measurements and a Peltier-cooled CCD for spectral detection. A super notch filter with lower cutoff at 50 cm^{-1} is used for Rayleigh line rejection.

3. Results and discussions

Figure 1 shows the room temperature Raman spectrum of $La_{1-x}Sr_xMnO_3$ ($x = 0.0$, 0.05, 0.1, 0.3, 0.5) with 488 and 632.8 nm excitation wavelengths in parallel (xx) and cross-polarization (xy) mode. The parallel polarized spectra show three dominant phonon modes (300, 490 and 610 cm^{-1}) present in the system. For a cubic perovskite structure no phonon mode is Raman-active and it is the orthorhombic or rhombohedral distortion that gives rise to Raman-active phonon modes. In an orthorhombic *Pnma* space group 60 optical modes [15] are allowed, out of which only 24 are Raman-active. The most interesting bands are those which occur at 490 and 613 cm^{-1}. These bands are typical of the insulating high-temperature phases of all disordered manganites, almost independent of the averaged crystallographic long-range symmetry (orthorhombic or rhombohedral) and on the element on the rare-earth site (La, Nd, Pr...). These bands are related to the JT octahedral distortions [16]. In the case of undoped compounds with orthorhombic structure the JT distortions are static and ordered. These bands are ordinary Raman-allowed modes of bending and stretching of Mn–O bonds, respectively. In the case of dynamical (in doped manganites) or non-spatially coherent JT distortion (in the case of rhombohedral structure) they could be considered as either 'forbidden'

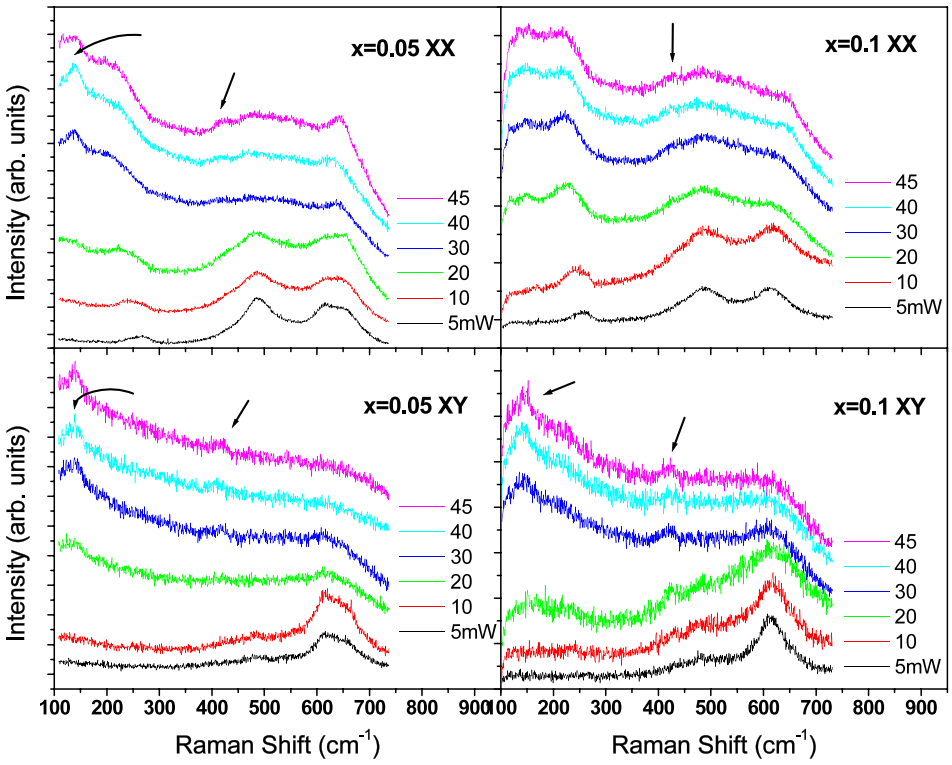

Figure 2. Raman spectra of $La_{1-x}Sr_xMnO_3$ single crystals at various incident laser powers (mW at the laser head) $x = 0.05$ (left panel) and $x = 0.1$ (right panel); collected in parallel (xx) and cross-polarization (xy) mode using 488 nm at room temperature. The spectra are shifted upwards for clarity. The arrow denotes the extra peaks seen with increasing laser power that is a signature of the appearance of metallic state in nature.

modes or disorder-induced bands of phonon density-of-states origin [17]. In the former case the linewidth of these bands is a measure of the mean lifetime of the JT distortions, while in the latter case the intensity of the bands is a measure of the displacements of oxygen atoms from their nominal sites in the averaged structure. The intensity of these bands is found to be higher in orthorhombic structure than compared to rhombohedral structure, giving further strength to the above arguments. The intensity and width of these bands represent the deviation from the perfect cubic structure and in turn these bands are representations of the Jahn–Teller contribution present in the system. The Raman spectra of figure 1 show that these JT peaks decrease with increasing x and had very little contribution at and above $x = 0.3$. Incidentally, for $x \geqslant 0.3$ samples small peaks appear at ∼140 and ∼425 cm^{-1} which were absent for lower doped samples. Thus these two new peaks can also be considered as a signature of diminishing Jahn–Teller distortion. Many researchers attributed broadening of the JT-induced peaks with increasing doping concentration to the site disorder-induced effects [16, 18]. However, appearance of new peaks makes one think of other possibilities. It is worth noting here that the peaks are more intense when probed with 632.8 nm wavelength in comparison to that when probed with 488 nm wavelength. Similar trends have been observed in resonant Raman studies by many workers before and are attributed to resonance effects [19].

Figure 2 shows the Raman spectra of $x = 0.05$ and 0.10 samples with increasing laser power ($\lambda = 488$ nm). It is interesting to note that the two JT-induced peaks showed decreasing intensity and broadening with increasing laser power, and above 30 mW of incident laser power the peaks were nearly non-existent. It is worth mentioning here that the laser power mentioned here is the peak power at the CW laser head. At the sample the power is expected to be reduced down to less than 30% due to several optical elements it interacts with before falling on the sample. At high laser powers (>20 mW) a small peak around 425 cm^{-1} and another peak at around 145 cm^{-1} were also visible. In other words, at higher incident laser power the Raman spectra for $x = 0.05$ and 0.10 samples resembled that of the $x = 0.3$ sample spectra taken at normal laser power (<10 mW) (see figure 1). If one looks at the phase diagram of $La_{1-x}Sr_xMnO_3$ it is seen that the samples show an insulating ground state up to $x = 0.16$ that becomes a ferromagnetic metallic state for higher doping. Another clue comes from the comparison of temperature-dependent Raman spectra of $x = 0.1$ (ferromagnetic insulator at low temperature) and $x = 0.5$ single crystal (ferromagnetic metal at and below room temperature) that is shown in figures 3(a) and (b), respectively. One can see that for the insulating sample ($x = 0.1$) as the temperature is reduced the JT peaks at 490 and 611 cm^{-1} show increasing intensity. On the other hand, there is no gain in intensity for these peaks for the metallic sample ($x = 0.5$). Raman bands at ∼425 and ∼140 cm^{-1} rather gain strength as the temperature is reduced for the $x = 0.5$ sample. From these observations one can conclude that the metallic state in these samples is reflected in the Raman spectra as total reduction of JT-distortion-induced bands along with the appearance of peaks at ∼425 and ∼140 cm^{-1}. Similar

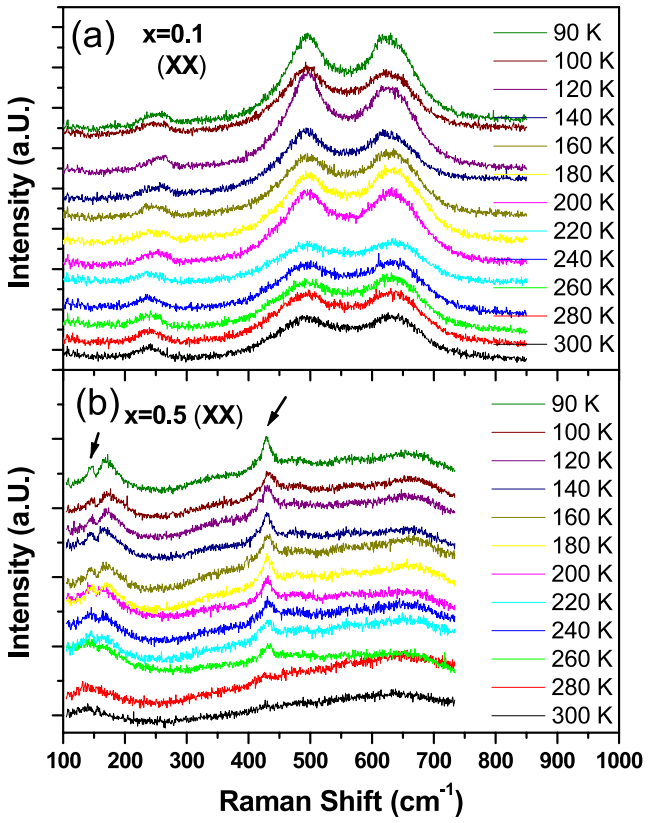

Figure 3. Temperature evolution of Raman spectra (a) $x = 0.1$ and (b) $x = 0.5$ single crystals collected in parallel (xx) polarization mode using 488 nm. The spectra are shifted upwards for clarity. The arrow denotes the extra peaks seen at ∼140 and 425 cm^{-1} with decreasing temperature only in the $x = 0.5$ metallic sample.

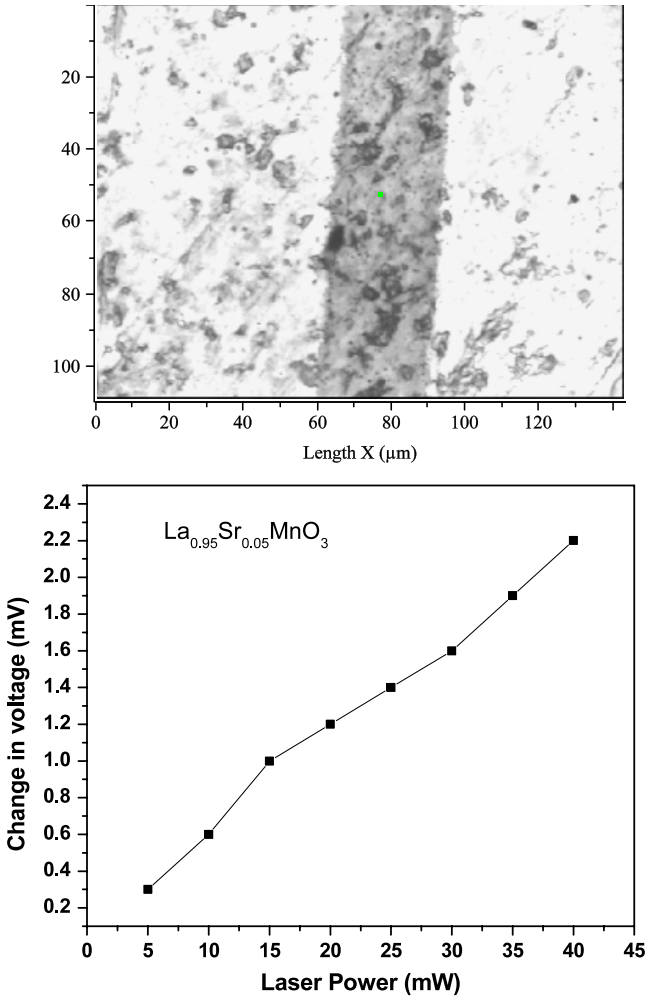

Figure 4. Effect of laser power on the conductivity of the $x = 0.05$ single crystal. A constant current of 1 mA (50 mV) was applied across a pair of electrodes that are 20 μm apart (top panel) and the drop in voltage is plotted as a function of increasing laser power.

behaviour was reported earlier in reference [17, 20] and seen in one of our studies on epitaxial thin films [21].

Raman observations for the $x = 0.05$ and 0.1 samples showed the common trend of pushing the system from insulating state to metallic state with increasing laser power. This encouraged us to carry out conductivity experiments as a function of increasing laser power. In the present case the laser is focused to ∼1 μm and hence it was found essential to make conductivity contacts across few micron distances to monitor the I–M transition for observing the photo-induced conductivity changes. The minimum gap that could be achieved in our laboratory was 20 μm. The laser source for Raman measurements was used for excitation and conductivity and Raman signals were measured simultaneously. The 488 nm (2.53 eV) laser was mainly used with increasing power from 5 to 45 mW. Two pairs of silver electrodes were vacuum-evaporated onto the surface of the sample. The pair of electrodes was separated by a straight 20 μm gap. A constant current source in the form of a multimeter was connected between one pair of electrodes while the voltage across the other two electrodes was monitored by a sensitive digital voltmeter. A current of 1.0 mA was kept constant between the current leads, giving a voltage difference of 50 mV for the $x = 0.05$ sample. The voltage decreased as the laser light was switched on and its value decreases further with increase in incident laser power. The change in voltage as a function of increasing laser power is shown in figure 4. This change in voltage is due to the I–M transition induced by illuminating the tiny (∼1 μm) area of the gap between the contacts (20 μm). It is observed that even for very small laser powers, 5–10 mW, the conductivity has shown a small measurable change. The Raman experiments with increasing laser power were repeated at 100 and 200 K with 488 nm excitation wavelength for the $x = 0.05$ and 0.1 samples. The photo-induced changes were found to be less prominent at lower temperatures for both samples.

The most important observation of these experiments is the reversible change of the I–M transition. It was observed that, as soon as the laser was turned off, the conductivity comes back to the original value. The experiment of turning on and off the incident laser was repeated several times on the same spot and the behaviour of conductivity and Raman spectra was observed. The behaviour was found perfectly reproducible in both the measurements confirming the perfect reversible behaviour of the I–M transition occurring locally. With the help of an optical camera the sample surface where the laser was focused was also checked and found visually unchanged.

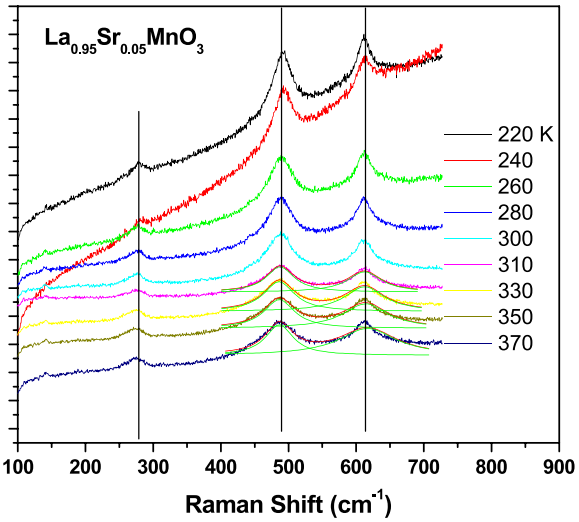

Figure 5. High-temperature evolution of Raman spectra of $x = 0.05$ sample collected using 488 nm excitation laser at normal power.

The natural question which first needs to be addressed is the contribution of the heating effect due to incident laser power in both Raman measurements as well as conductivity measurements. To address this question we carried out a number of measurements. Firstly Stokes and antiStokes measurements were carried out as a function of incident laser power and the intensity of Stokes and antiStokes lines was measured for a $LaMnO_3$ single crystal. This sample was chosen because it gives relatively many well-behaved peaks enabling more accurate fitting and extraction of the intensity ratio. The intensity ratio confirmed that the rise in temperature in this material is not more than 10 °C. As such the Stokes:antiStokes ratio method is accurate to a few tens of degrees and hence other attempts were also made to measure the rise in temperature. The temperature variation of a $LaMnO_3$ single crystal was carried out from 90 to 350 K and the line position and width were obtained as a function of temperature. From this change in the Raman band position and width, the per degree rise in temperature was estimated. The Raman bands with varying laser power were then compared for the same sample and from this experiment it was also confirmed that the change in temperature for maximum laser power (45 mW) was not more than ∼10 °C. Similar experiments of laser power variation were carried out at 5 °C below the transition temperature on a single crystal $SrTiO_3$ substrate. It shows a well-behaved transition from a cubic to tetragonal state below ∼105 K. The argument was if the local rise in temperature is more than 5 °C the signature of phase transition in Raman spectra should vanish with increasing laser power. However, the experiments retained the signatures of transformed phase, confirming again for $SrTiO_3$ that the temperature rise is not more than 5 °C. Finally the temperature-dependent Raman spectra was collected for the $x = 0.05$ sample from 220 to 370 K, which is shown in figure 5. This figure clearly shows that even at 370 K, which is 70 °C higher than room temperature, the sample showed well-behaved JT-induced peaks. These peaks showed normal broadening and softening due to the rise in temperature.

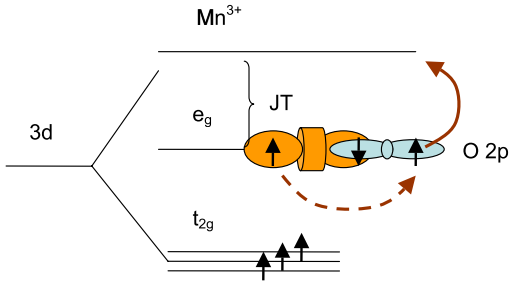

Figure 6. Schematics of impulsive stimulated Raman scattering photo-excitation in $La_{1-x}Sr_xMnO_3$. A 2.53 eV energy optical photon excites a transition between the Jahn–Teller split e_g states at the Mn 3+site mediated by the O 2p states. In this process a electron jumps from the O 2p state to the upper e_g level and simultaneously an electron from the lower e_g level gets transferred to the O 2p state.

From this it is estimated that for completely diminishing the JT peaks the sample temperature needs to be increased at least by 400 °C. A temperature rise due to the incident laser to such a high value is unbelievable. The appearance of new peaks with increasing laser power indicates that the effect cannot be merely due to thermal disorder. In the case of increasing thermal disorder well-defined peaks are not expected to emerge. The normal resistivity measurements for the $x = 0.05$ and 0.1 were carried out with the same contacts from 350 down to 5 K. From this, the expected drop in resistance, for a 5 °C rise in temperature, was calculated. This change in resistance at room temperature due to the possible rise of sample temperature on laser heating is found to be less than 25% when compared to the resistance drop found in laser-induced conductivity experiments. In the photo-induced conductivity experiments two kinds of responses were noted. First an instantaneous drop in resistance upon laser shining followed by a slow response that lasted for several minutes. The slow response is attributed to sample temperature rise, as a thermal shock requires some time to spread in these nearly insulating samples. The fast response is attributed to the photo-induced I–M phase transition.

It is worth noting here that the change of insulator to metallic state cannot be interpreted in terms of melting of the charge order state and of the collapse of the 0.3 eV insulating gap, as suggested in $Pr_{0.7}Ca_{0.3}MnO_3$ in previous reports [22] as, in the present case, the charge ordered state is not present at all. It is also needed to consider that in the present case a CW laser is used that delivers an average power of 45 mJ s^{-1} which is 10 orders smaller than the power delivered per second by a pulsed laser. The effect is also localized to a 1 μm spot while the gap was 20 μm. If we consider an absorption of 1 μm in the material for 488 nm light then the change in resistance for the 1 μm diameter particle is at least 10^{-2} times as a result of photo-excitation.

The possible photo-excitation mechanisms are shown in figure 6. The Mn^{3+} has $3t_{2g}$ electrons and one e_g electron. By virtue of its character the e_g electrons have electron density along the axes of the unit cell and hence have strong hybridization with the neighbouring oxygen 2p shell. On the other hand, the t_{2g} electrons have electron density between the unit cell axes and hence they have very weak hybridization

with the neighbouring oxygen 2p shell that can be neglected. The optical conductivity studies showed strong enhancement around 2 and 4.5 eV that were attributed to JT resonance and charge transfer resonance [19, 23, 24]. The e_g band of the Mn^{3+} ion splits into e_g^1 and e_g^2 bands due to coherent static JT distortion present in the orthorhombic $LaMnO_3$. The e_g^1 band should have strong overlap with the O 2p band due to strong hybridization, while the e_g^2 band forms the lowest-lying empty conduction band [23]. The bandgap between this empty conduction band formed by the e_g^2 band and the highest level valence band formed by overlap of e_g^1 with the O 2p is the JT bandgap responsible for the insulator character of this material. For Mn^{4+} ions the e_g band is completely empty and hence the JT gap is non-existent. Thus with increasing Mn^{4+} ion concentration as a function of doping concentration x, the JT gap collapses and the system is becoming metallic once the percolation threshold for doping is reached.

Figure 6 shows the possible photo-excitation mechanisms when a 2.53 eV photon is impinged on the material. There are only two channels available for the photo-excitation that will preserve charge neutrality at the 'Mn' site [24]. The first channel corresponds to excitation of an electron from the t_{2g} level to the e_g^2 level. This d–d transition is not allowed by the dipole selection rule and hence has to be mediated by the O 2p orbitals. As the overlap of t_{2g} orbitals with O 2p is very small and the crystal field splitting is expected to be at least 3 eV or more this channel can be safely neglected. The other possible channel is the transfer of an electron from the e_g^1 level to the e_g^2 level that is crossing the JT gap mediated through the O 2p. Naturally this mechanism is possible only at Mn^{3+} sites. Here the upper unoccupied e_g state is populated by photo-excitation of an electron from the O 2p state and simultaneously an electron decays from the occupied e_g level to the O 2p state. Polli *et al* has referred to this process as impulsive stimulated Raman scattering (ISRS) [12]. This excitation strongly couples with the JT distortion and is instrumental in melting it. This observation is consistent with the Raman results shown in figures 1 and 2 where JT distortion is strongly suppressed with increasing incident laser power. The reversible or non-persistent nature of the I–M transition further supports the excitation–de-excitation nature of the involved process. The electron that is populated in the e_g^2 band is now a conduction electron and should increase the conductivity significantly. Thus the conductivity increase is related to the extra charge carriers that were generated in the conduction band by the photo-excitation. The JT bandgap vanishes for metallic samples (as observed in our Raman measurements) and hence an incident laser photon of 2.53 eV has no effect on the conductivity.

Millis *et al* [5] had earlier showed that the double exchange mechanism proposed by Zener *et al* that is based on the large Hund coupling between e_g and t_{2g} electrons alone is not sufficient to explain the CMR. It is suggested that contributions arising from dynamic JT splitting should also be included. Our observations clearly bring out the validity of this argument.

In conclusion, a photo-induced insulator to metal transition is observed in a $La_{1-x}Sr_xMnO_3$ single crystal. The observation is well supported by Raman measurements. It is clearly shown that the JT gap vanishes due to a photo-induced transition of a e_g electron that is coupled to the change in the conductivity. The role of subtle interplay of charge and lattice degrees of freedom in the metal–insulator transition is established.

Acknowledgments

The authors gratefully acknowledge Dr P Chaddah for fruitful discussions and input. One of us (AVN) thanks the Indian Nation Science Academy, New Delhi for financial support. AD would like to gratefully acknowledge CSIR, New Delhi for an SRF fellowship.

References

[1] Campbell A J, Balakrishnan G, Lees M R, Paul D McK and McIntyre G J 1997 *Phys. Rev.* B **55** R8622
[2] Asamitau A, Moritomo Y, Tomioka Y, Arima T and Tokura Y 1995 *Nature* **373** 407
[3] Oleaga A, Salazar A, Prabhakaran D and Boothroyd A T 2004 *Phys. Rev.* B **70** 184402
Imada M, Fujimori A and Tokura Y 1998 *Rev. Mod. Phys.* **70** 1039
[4] Rini M, Tobey R, Dean N, Itatani J, Tomioka Y, Tokura Y, Schoenlein R W and Cavalleri A 2007 *Nature* **449** 72
[5] Millis A J, Littlewood P B and Shraiman B I 1995 *Phys. Rev. Lett.* **74** 5144
[6] Dagotto E 2005 *Science* **309** 257
[7] Mathur N and Littlewood P 2003 *Phys. Today* **56** 25
[8] Rao C N R and Raveau B (ed) 1998 *Colossal Magnetoresistance Charge-ordering and Related Aspects of Manganese Oxide* (Singapore: World Scientific)
[9] Kiryukhin V, Casa D, Hill J H, Keimer B, Vigliante A, Tomioka Y and Tokura Y 1997 *Nature* **386** 813
[10] Fiebig M, Miyano K, Tomioka Y and Tokura Y 1998 *Science* **280** 1925
[11] Miyano K, Tanaka T, Tomioka Y and Tokura Y 1997 *Phys. Rev. Lett.* **78** 4257
[12] Polli D, Rini M, Wall S, Schoenlein R W, Tomioka Y, Tokura Y, Cerullo G and Cavalleri A 2007 *Nat. Mater.* **6** 643
[13] Asamitsu A, Tomioka Y, Kuwahara H and Tokura Y 1997 *Nature* **388** 50
[14] Prabhakaran D, Coldea A I, Boothroyd A T and Blundell S J 2002 *J. Cryst. Growth* **237–239** 806
[15] Iliev M N, Abrashev M V, Laverdiere J, Jandl S, Gospodinov M M, Wang Y-Q and Sun Y-Y 2006 *Phys. Rev.* B **73** 064302
[16] Iliev M N and Abrashev M V 2001 *J. Raman Spectrosc.* **32** 805
[17] Iliev M N, Abrashev M V, Popov V N and Hadjiev V G 2003 *Phys. Rev.* B **67** 212301
[18] Iliev M N, Abrashev M V, Lee H-G, Popov V N, Sun Y Y, Thomsen C, Meng R L and Chu C W 1998 *Phys. Rev.* B **57** 2872
[19] Kruger R, Schulz B, Naler S, Rauer R, Budelmann D, Backstrom J, Kim K H, Cheong S-W, Perebeinos V and Rubhausen M 2004 *Phys. Rev. Lett.* **92** 97203
[20] Bjornsson P, Rubhausen M, Backstrom J, Kall M, Eriksson S, Eriksen J and Borjesson L 2000 *Phys. Rev.* B **61** 1193
[21] Dubey A, Sathe V G and Rawat R 2008 *J. Appl. Phys.* **104** 113530
[22] Fiebig M, Miyano K, Tomioka Y and Tokura Y 1999 *Appl. Phys. Lett.* **74** 2310
[23] Jung J H, Kim K H, Eom D J, Noh T W, Choi E J, Yu Jaejun, Kwon Y S and Chung Y 1997 *Phys. Rev.* B **55** 15489
[24] Jung J H, Kim K H, Noh T W, Choi E J and Yu Jaejun 1998 *Phys. Rev.* B **57** R11043